

Preferential dipeptide incorporation of *Porphyromonas gingivalis* mediated by proton-dependent oligopeptide transporter (Pot)

Yuko Ohara-Nemoto^{1,*}, Mohammad Tanvir Sarwar¹, Yu Shimoyama², Takeshi Kobayakawa¹, and Takayuki K. Nemoto¹

¹Department of Oral Molecular Biology, Course of Medical and Dental Sciences, Nagasaki University Graduate School of Biomedical Sciences, Nagasaki 852-8588, Japan

²Division of Molecular Microbiology, Department of Microbiology, Iwate Medical University, 1-1-1 Idai-dori, Yahaba 028-3694, Japan

*Corresponding author: Yuko Ohara-Nemoto, Department of Oral Molecular Biology, Nagasaki University Graduate School of Biomedical Sciences, 1-7-1 Sakamoto, Nagasaki 852-8588, Japan
Tel: +81-95-819-7643; Fax: +81-95-819-7642; email: oharanemoto@gmail.com

One sentence summary: *Porphyromonas gingivalis* preferentially incorporates dipeptides via proton-dependent oligopeptide transporter.

Keywords: dipeptide; dipeptidyl-peptidase; oligopeptide transporter; *Porphyromonas gingivalis*; proton-dependent oligopeptide transporter; serine/threonine transporter

Topics: amino acid incorporation; dipeptide production; resazurin assay

Abstract

Multiple dipeptidyl-peptidases (DPPs) are present in the periplasmic space of *Porphyromonas gingivalis*, an asaccharolytic periodontopathic bacterium. Dipeptides produced by DPPs are presumed to be transported into the bacterial cells and metabolized to generate energy and cellular components. The present study aimed to identify a transporter responsible for dipeptide uptake in the bacterium. A real-time metabolic analysis demonstrated that *P. gingivalis* preferentially incorporated Gly-Xaa dipeptides, and then, single amino acids, tripeptides, and longer oligopeptides to lesser extents. Heterologous expression of the *P. gingivalis* serine/threonine transporter (SstT) (PGN_1460), oligopeptide transporter (Opt) (PGN_1518), and proton-dependent oligopeptide transporter (Pot) (PGN_0135) genes demonstrated that *Escherichia coli* expressing Pot exclusively incorporated Gly-Gly, while SstT managed Ser uptake and Opt was responsible for Gly-Gly-Gly uptake. Dipeptide uptake was significantly decreased in a *P. gingivalis* Δpot strain and further suppressed in a Δpot - Δopt double-deficient strain. In addition, the growth of the Δpot strain was markedly attenuated and the Δpot - Δopt strain scarcely grew, whereas the $\Delta sstT$ strain grew well almost like wild type. Consequently, these results demonstrate that predominant uptake of dipeptide in *P. gingivalis* is mostly managed by POT. We thus propose that Pot is a potential therapeutic target of periodontal disease and *P. gingivalis*-related systemic diseases.

INTRODUCTION

Porphyromonas gingivalis, an asaccharolytic Gram-negative anaerobe, is a keystone pathogen in chronic periodontitis, a highly prevalent type of chronic inflammation of periodontal tissues. This disease is the main cause of tooth loss in adults, which decreases the quality of life especially in the elderly. In addition, a large number of epidemiological and molecular-based studies have shown a keen association of chronic periodontitis and type 2 diabetes mellitus accounted for the involvement of inflammation and bacterial pathogens like lipopolysaccharide (Grossi and Genco 1998; Lalla and Papapanou 2011). We recently reported a more direct commitment of periodontopathic bacteria to the disease in which bacterial dipeptidyl-peptidase (DPP) 4 modulates blood glucose level through the degradation of incretin peptides, glucagon-like peptide 1 (GLP-1) and

glucose-dependent insulintropic polypeptide (GIP) (Ohara-Nemoto *et al.* 2017). Furthermore, *P. gingivalis* has been recently detected in the brain, suggesting its association with neurodegeneration in Alzheimer's disease patients (Dominy *et al.* 2019). Therefore, it is important to elucidate the bacterial metabolic process for disease prevention and care of *P. gingivalis*-related systemic as well as oral diseases.

P. gingivalis growth is not supported by carbohydrates but by proteinaceous nutrients, and then the bacterium exclusively utilizes amino acids as its carbon and energy sources (Seddon *et al.* 1988). Previous studies suggested that most proteinaceous nutrients are incorporated as dipeptides into bacterial cells, since the production of end products such as methyl mercaptan and ammonia is significantly accelerated by the addition of dipeptides (Tang-Larsen *et al.* 1995; Takahashi and Sato 2001). In accord with these findings, *P. gingivalis* characteristically possesses four kinds of periplasmic dipeptidyl-peptidases (DPPs) that liberate dipeptides from the non-modified N-termini of polypeptides, in contrast to a trace of aminopeptidase activity (Nemoto and Ohara-Nemoto 2016b; Ohara-Nemoto *et al.* 2018). DPP4 preferentially cleaves a peptide bond on the C-terminal side of penultimate Pro from the N-terminus (P1 position) (Kiyama *et al.* 1998; Banbula *et al.* 2000) and P1 Ala with a lesser extent (Mentlein, Gallwitz and Schmidt 1993). DPP4 from *P. gingivalis* degrades GLP-1 and GIP same as the mammalian entity, resulting in elevation and prolongation of postprandial hyperglycemia in the mouse model (Ohara-Nemoto *et al.* 2017). Both DPP5 (Ohara-Nemoto *et al.* 2014) and DPP7 (Banbula *et al.* 2001) are preferential for P1 hydrophobic residues, though DPP7 prefers hydrophobic N-terminal (P2-position) residues (Nemoto *et al.* 2018) and DPP5 has no such preference (Rouf *et al.* 2013). Finally, DPP11 is specific for P1 acidic residues, Asp and Glu (Ohara-Nemoto *et al.* 2011). Accompanying with these DPPs, *P. gingivalis* expresses prolyl tripeptidyl-peptidase A (PTP-A) (Banbula *et al.* 1999) and acylpeptidyl oligopeptidase (AOP) (Nemoto *et al.* 2016a) in the periplasmic space, which provide oligopeptides acceptable for DPPs. These characteristic features of dipeptide production and possible utilization let us presume that amino acid nutrients are transported mainly as a dipeptidyl form via a plasma membrane transporter. In the present study, we aimed to identify the transport molecule responsible for dipeptide uptake in *P. gingivalis*.

METHODS

Bacterial growth conditions

P. gingivalis ATCC 33277 were grown at 37°C anaerobically (80% N₂, 10% CO₂, 10% H₂) in Anaerobic Bacterial Culture Medium (ABCM) broth (EIKEN Chemical, Tochigi, Japan) supplemented with 0.5 µg mL⁻¹ of menadione without or with 10 µg mL⁻¹ of ampicillin and/or erythromycin. To measure bacterial growth, bacterial cells were collected in an early stationary phase and resuspended in the broth to adjust to 0.2 at A₆₀₀. Cultures in a 96-well plate were monitored by measuring A₆₀₀. Growth was also measured by spotting 2 µL of 10-time serially diluted bacterial suspensions from a concentration of 10⁷ cfu 2 µL⁻¹ on ABCM agar plates containing 0.5 µg mL⁻¹ of menadione and 5% sheep blood (blood agar plates). *E. coli* XL-1 blue and *Streptococcus anginosus* NCTC 10713 were cultured aerobically at 37°C in Luria-Bertani (LB) broth and brain heart infusion broth, respectively.

Substrate uptake assay

Transporter activities were evaluated by a real-time measurement of bacterial metabolic activity using alamarBlue Cell Viability Reagent composed of resazurin (Thermo Fisher Scientific, Waltham, USA), according to previous reports (Shiloh, Ruan and Nathan 1997; Ishiguro *et al.* 2015) with slight modifications. In brief, bacterial cells precultured to A₆₀₀ of 0.8 were harvested, washed twice with ice-cold PBS, and then suspended in 50 mM HEPES, pH 7.5, to A₆₀₀ of 0.3. The reagent was added to the cell suspensions giving a final concentration of 2.5 mM and incubated at 25°C for 5 min. Measurement was started by the addition of an aliquot (40 µL) of the bacterial cell suspension to a reaction mixture (final 200 µL) composed of 50 mM HEPES without or with either 10 mM single amino acids, 5 mM dipeptides, 5 mM each of two kinds of amino acids, or equivalent amounts of peptidyl compounds in an OptiPlate-96F (PerkinElmer). Fluorescence intensity with excitation at 550 nm and emission at 585 nm was measured every five min after two sec-shaking for 30 min with a DTX 800 Multimode Detector (Beckman Coulter). Fluorescence intensity (n = 4) was subtracted by that without a substrate, then the resulting figures represented genuine incorporation and metabolism mediated by each substrate. Amino acids,

Gly-Gly, Gly-Gln, Gly-Leu, Gly-Glu, polyE750, and polyE1500 were purchased from Sigma-Aldrich. Gly-Pro, Glu-Glu, and GGG were from Peptide Institute (Ibaraki, Japan), acetyl (Ac)-Gly-Leu and GGP from Bachem (Bubendorf, Switzerland), and Gly-Ser from Tokyo Chemical Industry.

Expression of transporter proteins in *E. coli*

The serine/threonine transporter (SstT) (PGN_1640), putative oligopeptide transporter (Opt) (PGN_1518), and putative H⁺/peptide symporter (alias proton-dependent oligopeptide transporter, Pot) (PGN_0135) genes were amplified by PCR with genomic DNA and an appropriate set of primers (Supplementary Table S1). PCR products were cloned into pTrcHis2-TOPO and the constructs were verified by sequencing. *E. coli* XL1-Blue harboring the plasmid was cultured in LB broth supplemented with 75 µg mL⁻¹ of ampicillin at 37°C for 16 h, then diluted 3-fold with LB broth and the culture was continued. After 1-h culture, bacterial cells were divided into two aliquots with or without 0.2 mM IPTG, and then further cultured at 30°C. After 3 h, bacterial cells were harvested and washed with ice-cold PBS and then subjected to further analyses.

Construction of *P. gingivalis* strains disrupting transporter genes

P. gingivalis strains with disrupted transporter genes were constructed by homologous recombination (Table 1). In short, to construct NDP700 Δ *sstT* (*sstT::cepA*), DNA fragments from both the 5'- and 3'-parts of the PGN_1640 gene were PCR amplified with primers (Supplementary Table S1). A *cepA* fragment flanked with parts of PGN_1640 was amplified with primers using pCR4-TOPO as a template. Integrated PCR was performed with a mixture of the three fragments with a set of primers (PGN1640-5F1 and 3R-comp-2-PGN1640), then an obtained DNA fragment was introduced into *P. gingivalis* by electroporation. Gene-disrupted strains were selected on blood agar plates containing 10 µg mL⁻¹ of ampicillin. Similarly, NDP800 Δ *opt* (*opt::cepA*) and NDP900 Δ *pot* (*pot::cepA*) were generated. For the second gene disruption, DNA fragments of the *opt* and *pot* genes were inserted with an erythromycin-resistant gene cassette (*ermF ermAM*) derived from pYKP301 by integrated PCR, and then the obtained fragments were introduced into the single-gene deficient

mutants. Double transporter-gene disrupted strains were selected in the presence of 10 $\mu\text{g mL}^{-1}$ each of ampicillin and erythromycin.

Immunoblot analysis

E. coli cells (1 mL) were harvested and lysed in SDS-sample buffer (0.1 mL) containing 5 mM dithiothreitol and 10 μL of GLASSMILK suspension (MP Biomedicals) to remove genomic DNA. For *P. gingivalis* cells, 50 μM tosyl-L-lysyl-chloromethane hydrochloride, 3 μM E64, and 10 $\mu\text{g mL}^{-1}$ of leupeptin were further added to inhibit protease activities. After heating and centrifugation, proteins were separated by SDS-PAGE and transferred to a polyvinylidene difluoride membrane. The membrane was incubated with 1% skim milk in PBS containing 0.05% Tween 20 and 0.05% Triton X-100. *P. gingivalis* transporters were detected using mouse anti-hexahistidine Ig followed by alkaline phosphatase-conjugated anti-mouse IgG, and visualized with 5-bromo-4-chloro-3-indolyl phosphate and nitro blue tetrazolium (Promega). A rainbow marker and low molecular weight markers were purchased from GE Healthcare. Anti-*P. gingivalis* Pot Ig was produced against a synthesized peptide (CM¹³⁴YDNDTYRDKR¹⁴⁴) using a Wistar rat. Non-endogenous 'C' was added to facilitate conjugation to a hapten scaffold. After blocking, the membrane was incubated with anti-Pot Ig followed with horseradish peroxidase-conjugated anti-rat IgG, and then the bands were visualized with Western BLoT Ultra Sensitive HPR Substrate (Takara Bio, Kusatsu, Japan). Protein concentration was determined with the Coomassie Brilliant Blue dye method (Promega) using bovine albumin as the standard.

Amino acid sequence alignment and 3D homology modeling

Amino acid sequences of bacterial POT members were aligned using Clustal W (Larkin *et al.* 2007). A phylogenetic tree was created by PhyML of the SeaView multiplatform with the default setting (Gouy, Guindon and Gascuel 2010). Homology modeling of the 3D structure was generated by Phyre2 (Kelley *et al.* 2015) and visualized using the PyMOL Molecular Graphics System, Ver 2.0 (Schrödinger).

RESULTS AND DISCUSSION

Dipeptide incorporation in *P. gingivalis*

P. gingivalis holds a series of DPPs together with their supporting exopeptidases, PTP-A and AOP, while aminopeptidase activities are scant. These specialized features for producing dipeptides seem to be beneficial for the bacterium to acquire its niche in the oral cavity (Nemoto and Ohara-Nemoto, 2020). Since information on amino acid incorporation of *P. gingivalis* is limited, we firstly examined single amino acid uptake in *P. gingivalis* by real-time measurement of the metabolic activity (Shiloh, Ruan and Nathan 1997; Ishiguro *et al.* 2015). The higher increase in fluorescence intensity was obtained with Gly, Leu, Ser (Fig. 1), and Thr (data not shown) than Gln, Pro, Glu (Fig. 1), and other amino acids (data not shown). Because Gly provided a high fluorescence intensity and six Gly-Xaa dipeptides and GGG were commercially available, we subsequently used these glyceryl compounds. In addition, Glu-Glu and Glu oligopeptides (polyE750 and polyE1500), which have been previously used for the bacterial metabolic study (Takahashi and Sato, 2001), were also tested.

As shown in Fig. 1A, fluorescence intensity increased linearly for 30 min, indicating that substrates incorporated into the bacterial cells were readily metabolized to produce reducing molecules including NADH. The increase was significant in the presence of Gly-Gly and Gly-Leu as compared to those with equivalent amounts of Gly, Leu, and a mixture of Gly and Leu. In contrast, *Strep. anginosus* and *E. coli*, saccharolytic bacteria that possess no DPPs, did not show obvious differences in the intensity among the substrates at 30 min (Fig. 1B). These results indicate that the increase in fluorescence intensity primarily reflects the incorporation efficiency of substrates as compared with the metabolic efficiency of each amino acid at least in *P. gingivalis*. Substrate preference of *P. gingivalis* was further examined (Fig. 1C). The results again demonstrated that *P. gingivalis* more preferentially incorporates dipeptides, particularly Gly-Gly, Gly-Ser, Gly-Gln, and Gly-Leu, while uptake of dipeptides composed of Pro and Glu seemed limited. The efficiency of incorporation of single amino acids (Gly, Ser, Leu), a combination of the two amino acids, and tripeptides GGG and GGP was 15 – 40% of that of Gly-Gly. The uptake of Gln, Glu, and Pro was limited. Although Gly-Leu was favorable, Ac-Gly-Leu was poorly incorporated (5% of Gly-Leu), uptake of Poly-Glu750 [(Glu)₆ as a major part] was scarce, and poly-Glu1500 [(Glu)₁₁₋₂₀] was not incorporated. Taken together, these results confirmed that *P. gingivalis* more

preferentially incorporates proteinaceous nutrients as dipeptidyl forms than single amino acids, tripeptides and longer oligopeptides.

Functional expression of *P. gingivalis* transporters in *E. coli*

P. gingivalis ATCC 33277 (Pg) possesses three candidates of amino acid transporter genes (Naito *et al* 2008): the serine/threonine transporter *sstT* (PGN_1640) encoding 412 amino acids with a predicted molecular mass of 41,951 (Dashper *et al.* 2001), the putative oligopeptide transporter *opt* (PGN_1518) encoding 659 amino acid residues with a molecular mass of 69,743, and the putative H⁺/peptide symporter (alias proton-dependent oligopeptide transporter) *pot* (PGN_0135) encoding 513 amino acids with a predicted molecular mass of 56,727. To elucidate their roles in substrate uptake, full-length of the three genes were expressed in *E. coli* as C-terminal hexahistidine tagged molecules (Table 1, Fig. 2). After induction, PgSstT was detected as a 28-kDa band, with 58- and 94-kDa and even larger bands. A small amount of 28-kDa SstT was observed without induction (Fig. 2A, lanes 1 and 2). PgOpt was expressed as a 46-kDa monomer with a 110-kDa dimer, and PgPot as 35-, 76- and 150-kDa bands. These findings suggest a polymerization tendency of the *P. gingivalis* transporters even under denaturing conditions.

Substrate uptake of *E. coli* expressing *P. gingivalis* transporters was examined with Ser, Gly-Gly, and GGG, since Ser is a major substrate for SstT (Dashper *et al.* 2001) and Gly-Gly and GGG recorded maximal incorporation in dipeptidyl and tripeptidyl forms, respectively (Fig. 1C). Inherent uptakes of *E. coli* cells without and with IPTG induction were subtracted from those values of the cells harboring expressing plasmids, resulting in the figures deduced by expression of *P. gingivalis* transporters. The uptake of Ser was significantly enhanced in *E. coli* expressing PgSstT, whereas those were negligible in both *E. coli* with PgOpt and PgPot (Fig. 2B). Incorporation of Gly-Gly was markedly increased in *E. coli* expressing PgPot after induction, while GGG uptake was enhanced in *E. coli*-PgOpt. A small GGG uptake observed in *E. coli*-PgPot was independent of induction. These results suggest that *P. gingivalis* transporters were functionally expressed in *E. coli*. As a result, it was concluded that Pot is predominantly responsible for dipeptide uptake, Opt for tripeptides, and SstT for amino acids in *P. gingivalis*.

Characteristics of *P. gingivalis* mutants with disrupted transporter genes

Single ($\Delta sstT$, Δopt , Δpot)- and double ($\Delta sstT$ - Δopt , $\Delta sstT$ - Δpot , Δopt - Δpot , Δpot - Δopt)-transporter gene-disrupted *P. gingivalis* strains were constructed (Table 1). Mutant strains were selected by antimicrobial resistances and gene disruption was further confirmed by PCR. The length of inserted *cepA* gene was 1,117 bp and that of *ermF-ermAM* was 2,179 bp, and then the amplified *sstT::cepA* fragment (1,925 bp) was observed in the $\Delta sstT$, $\Delta sstT$ - Δopt , and $\Delta sstT$ - Δpot strains (Fig. 3A, lanes 2, 5, and 6, respectively). The *opt::cepA* fragment (2,643 bp) was demonstrated in the Δopt and Δopt - Δpot (lanes 3 and 7, respectively), that of the *opt::ermF-ermAM* (3,705 bp) was in the $\Delta sstT$ - Δopt and Δpot - Δopt (lanes 5 and 8, respectively), that of the *pot::cepA* (2,458 bp) was present in the Δpot and Δpot - Δopt (lanes 4 and 8, respectively), and the *pot::ermF-ermAM* (3,520 bp) was in the $\Delta sstT$ - Δpot and Δopt - Δpot strains (lanes 6 and 7, respectively). Since NDP901 (Δpot - Δopt) exhibited a similar growth profile and substrate uptake tendency to those of NDP801 (Δopt - Δpot), the results from NDP801 are solely presented following.

P. gingivalis Pot was shown as the main 35-kDa band together with minor 76- and 150-kDa bands, the same as those of Pot molecules expressed in *E. coli* (Figs. 3B). Although all bands disappeared in the *pot* mutants, those amounts seemed to decrease in the $\Delta sstT$ - Δopt strain due to an unknown reason at present. The apparent molecular size of 35 kDa of Pot was smaller than the calculated value (molecular mass = 56,746) on SDS-PAGE, and this feature of membrane proteins has been commonly reported, such as *E. coli* Pot (Weitz *et al.* 2007).

Uptakes of five Gly-Xaa dipeptides and Glu-Glu were examined using the transporter-deficient strains (Fig. 3C). The $\Delta sstT$ mutant showed a profile similar to that of the wild type, confirming that SstT does not incorporate dipeptides. In contrast, dipeptide uptakes were significantly reduced in the Δpot strain (approx. 30 – 60 % each of that in the wild type). Since the Δpot strain maintained certain dipeptide uptake, other molecules such as Opt might function as a dipeptide transporter under these conditions. Unexpectedly, an enhanced dipeptide uptake (130%) was observed in the Δopt strain. These findings further suggested that the defect of *opt* is likely compensated by the expression of other molecules such as Pot, because of its involvement as an

adequate role in nutrient uptake. Among the double-deletion mutants, dipeptide uptake was not significantly altered in $\Delta sstT\text{-}\Delta opt$, and the $\Delta sstT\text{-}\Delta pot$ strain also exhibited incorporation of dipeptides, except for a significant decrease in Glu-Glu. In contrast, dipeptide uptake was markedly reduced in the $\Delta opt\text{-}\Delta pot$ strain. These observations again suggest that the defect of either *opt* or *pot* gene could be compensated by upregulation of another gene, while such compensation hardly occurred in the $\Delta opt\text{-}\Delta pot$ double-deficient mutant.

The growth of the *P. gingivalis* transporter-deficient strains was investigated in liquid and on blood agar plate cultures. As shown in Fig. 3D, the $\Delta sstT$ strain showed the least extent of growth retardation, further suggesting that uptake of single amino acids via SstT is rather limited and does not significantly contribute to bacterial metabolism and energy production. On the other hand, modest growth retardation was observed in the Δopt strain, while that was markedly attenuated in the Δpot strain with a prolonged lag phase. With blood agar plate culture (Fig. 3E), the weakness of the growth of the Δpot strain was reproduced. Furthermore, the growth of the $\Delta sstT\text{-}\Delta opt$ was more weakened than those of their single mutants, and the $\Delta opt\text{-}\Delta pot$ strain failed to grow except with the highest level of inoculation. These results indicate that dipeptide uptake mainly managed by Pot is most closely associated with bacterial growth and suggest that Opt appears to have a subsidiary role in substrate incorporation. SstT seemed to have the least role in the growth under these conditions.

Amino acid sequence comparison and 3D structure modeling of *P. gingivalis* Pot

The amino acid sequence of *P. gingivalis* Pot (PgPot) exhibits 29.6% similarity with that of *Geobacillus kaustophilus* Pot (GkPOT), followed by 29.2% to that of *Shewanella oneidensis* PepT_{so}, 27.7% to that of *E. coli* dipeptide and tripeptide permease B (DtpB), and 27.3% to that of *Streptococcus thermophilus* PepT_{st}, while the phylogenetic tree shows a closer kinship with *E. coli* DtpB than *S. oneidensis* PepT_{so} (Supplemental Fig. S1). The amino acid sequence alignment with other bacterial entities, in which 3D structures have been determined, indicates that identical amino acid residues are mainly located at the N-terminal half (Fig. 4). The conserved 'ExxER/K' motif in the POT members was shown to change to 'N¹⁶MGER²⁰' in PgPot, though Glu³² in GkPot has been reported to be essential for proton-driven uptake of substrates (Doki *et al.* 2013). KEGG orthologue search revealed that the 'NxGER' sequence is conserved in the members in the order *Bacteroidales* including

periodontopathic bacteria such as *Tannerella forsythia* and *Prevotella intermedia*, and gut indigenous bacteria such as *Bacteroides fragilis*, *Bacteroides thetaiotaomicron*, and *Alistipes onderdonkii*, as well as the species in the family *Porphyromonadaceae*. Because of the medical importance, it is interesting to examine whether amino acid substitutions in the conserved motif provides specific characteristics to *Bacteroidales* POT members.

Homology modeling of the 3D structure (471 of 513 residues, 92%) was generated with 100% confidence by the single highest scoring template of GkPot (Doki *et al.* 2013), showing that PgPot consists of the conserved N-bundle transmembrane regions (TM) 1–6 and C-bundle TM 7–12, with the α helix regions HA and HB (Fig. 5). The N- and C-bundles surround and form a large central cleft, thus providing a substrate-binding site. Since diverse substrate promiscuity is recognized as a characteristic feature of the POT members (Weitz *et al.* 2007; Ito *et al.* 2013; Newstead 2015), it is of interest to elucidate that the 3D structure and the substrate multispecificity of *P. gingivalis* Pot.

CONCLUSIONS

P. gingivalis preferentially incorporates dipeptides as nutritional amino acids, which is managed predominantly by Pot. The other two transporters, *i.e.*, Opt mainly responsible for tripeptides and SstT for single amino acids, play subsidiary roles in uptakes of nutritional amino acids. Bacterial growth was significantly retarded in the Δpot mutant, and the Δpot - Δopt double mutant scarcely grew under the present culture conditions. Thus, dipeptide production by DPPs and their uptake by Pot are conclusive molecular events in *P. gingivalis* for the entire metabolism and energy production. The present results indicate that the Pot molecule can be a potential drug target for the prevention and care of periodontal disease as well as *P. gingivalis*-related systemic diseases such as type 2 diabetes mellitus and Alzheimer's disease.

SUPPLEMENTARY DATA

Supplementary data are available at *FEMS* online.

ACKNOWLEDGMENTS

We are grateful for the technical assistance of Dr. T.T. Baba and Dr. T. Ono (Nagasaki University).

FUNDING

This study was supported by JSPS KAKENHI Grant Numbers 18K09557 (to Y.S.), 19K10045 (to T.K.N.), 19K10071 (to Y.O.-N.) and a grant from the Kyushu Dentist Association (to T.K.N.).

Conflicts of Interest. None declared.

REFERENCES

- Banbula A, Mak P, Bugno M *et al.* Prolyl tripeptidyl peptidase from *Porphyromonas gingivalis*. A novel enzyme with possible pathological implications for the development of periodontitis. *J Biol Chem* 1999;**274**:9246–52.
- Banbula A, Bugno M, Goldstein J *et al.* Emerging family of proline-specific peptidases of *Porphyromonas gingivalis*: purification and characterization of serine dipeptidyl peptidase, a structural and functional homologue of mammalian prolyl dipeptidyl peptidase IV. *Infect Immun* 2000;**68**:1176–82.
- Banbula A, Yen J, Oleksy A *et al.* *Porphyromonas gingivalis* DPP-7 represents a novel type of dipeptidylpeptidase. *J Biol Chem* 2001;**276**:6299–305.
- Dashper SG, Brownfield L, Slakeski N *et al.* Sodium ion-driven serine/threonine transport in *Porphyromonas gingivalis*. *J Bacteriol* 2001;**183**:4142–8.
- Doki S, Kato HE, Solcan N *et al.* Structural basis for dynamic mechanism of proton-coupled symport by the peptide transporter POT. *Proc Natl Acad Sci USA* 2013;**110**:11343–8.
- Dominy SS, Lynch C, Ermini F *et al.* *Porphyromonas gingivalis* in Alzheimer's disease brains: Evidence for disease causation and treatment with small-molecule inhibitors. *Sci Adv* 2019;**23**:eaau3333.

- Gouy M, Guindon S, Gascuel O. SeaView version 4: A multiplatform graphical user interface for sequence alignment and phylogenetic tree building. *Mol Biol Evol* 2010;**27**:221–4.
- Grossi SG, Genco RJ. Periodontal disease and diabetes mellitus: a two-way relationship. *Ann Periodontol* 1998;**3**:51–61.
- Ishiguro K, Washio J, Sasaki K *et al.* Real-time monitoring of the metabolic activity of periodontopathic bacteria. *J Microbiol Methods* 2015;**115**:22–6.
- Ito K, Hikida A, Kawai S, *et al.* Analysing the substrate multispecificity of a proton-coupled oligopeptide transporter using a dipeptide library. *Nat Commun* 2013;**4**:2502 doi: 10.1038/ncomms3502.
- Kelley LA, Mezulis S, Yates CM *et al.* The Phyre2 web portal for protein modeling, prediction and analysis. *Nat Protoc* 2015;**10**:845–58.
- Kiyama M, Hayakawa M, Shiroza T *et al.* Sequence analysis of the *Porphyromonas gingivalis* dipeptidyl peptidase IV gene. *Biochim Biophys Acta* 1998;**1396**:39–46.
- Lalla E, Papapanou PN. Diabetes mellitus and periodontitis: a tale of two common interrelated diseases. *Nat Rev Endocrinol* 2011;**7**:738–48.
- Larkin MA, Blackshields G, Brown NP *et al.* Clustal W and Clustal X version 2.0. *Bioinformatics* 2007;**23**:2947–8.
- Mentlein R, Gallwitz B, Schmidt WE. Dipeptidyl-peptidase IV hydrolyses gastric inhibitory polypeptide, glucagon-like peptide-1(7-36)amide, peptide histidine methionine and is responsible for their degradation in human serum. *Eur J Biochem* 1993;**214**:829–35.
- Naito M, Hirakawa H, Yamashita A *et al.* Determination of the genome sequence of *Porphyromonas gingivalis* strain ATCC 33277 and genomic comparison with strain W83 revealed extensive genome rearrangements in *P. gingivalis*. *DNA Res* 2008;**15**:215–25.
- Nemoto TK, Ohara-Nemoto Y, Bezerra GA *et al.* A *Porphyromonas gingivalis* periplasmic novel exopeptidase, acylpeptidyl oligopeptidase, releases N-acylated di- and tripeptides from oligopeptides. *J Biol Chem* 2016a;**291**:5913–25.
- Nemoto TK, Ohara-Nemoto Y. Exopeptidases and gingipains in *Porphyromonas gingivalis* as prerequisites for its amino acid metabolism. *Jpn Dent Sci Rev* 2016b;**52**:22–9.

- Nemoto TK, Ono T, Ohara-Nemoto Y. Establishment of potent and specific synthetic substrate for dipeptidyl-peptidase 7. *Anal Biochem* 2018;**548**:78–81.
- Nemoto TK, Ohara-Nemoto Y. Dipeptidyl-peptidases: Key enzymes producing entry forms of extracellular proteins in asaccharolytic periodontopathic bacterium *Porphyromonas gingivalis*. *Mol Oral Microbiol* 2020; doi: 10.1111/omi.12317.
- Newstead S. Molecular insights into proton coupled peptide transport in the PTR family of oligopeptide transporters. *Biochim Biophys Acta* 2015;**1850**:488–99.
- Ohara-Nemoto Y, Shimoyama Y, Kimura S *et al*. Asp- and Glu-specific novel dipeptidyl peptidase 11 of *Porphyromonas gingivalis* ensures utilization of proteinaceous energy sources. *J Biol Chem* 2011;**286**:38115–27.
- Ohara-Nemoto Y, Rouf SM, Naito M *et al*. Identification and characterization of prokaryotic dipeptidyl-peptidase 5 from *Porphyromonas gingivalis*. *J Biol Chem* 2014;**289**:5436–48.
- Ohara-Nemoto Y, Nakasato M, Shimoyama Y *et al*. Degradation of incretins and modulation of blood glucose levels by periodontopathic bacterial dipeptidyl peptidase 4. *Infect Immun* 2017;**85**(9):pii: e00277-17.
- Ohara-Nemoto Y, Shimoyama Y, Nakasato M *et al*. Distribution of dipeptidyl peptidase (DPP) 4, DPP5, DPP7 and DPP11 in human oral microbiota—potent biomarkers indicating presence of periodontopathic bacteria. *FEMS Microbiol Lett* .2018;**365**:doi: 10.1093/femsle/fny221.
- Rouf SM, Ohara-Nemoto Y, Ono T *et al*. Phenylalanine 664 of dipeptidyl peptidase (DPP) 7 and phenylalanine 671 of DPP11 mediate preference for P2-position hydrophobic residues of a substrate. *FEBS Open Bio* 2013;**3**:177–83.
- Seddon SV, Shah HN, Hardie JM *et al*. Chemically defined and minimal media for *Bacteroides gingivalis*. *Curr Microbiol* 1988;**17**:147–9.
- Shiloh MU, Ruan J, Nathan C. Evaluation of bacterial survival and phagocyte function with a fluorescence-based microplate assay. *Infect Immun* 1997;**65**:3193–8.
- Takahashi N, Sato T. Preferential utilization of dipeptides by *Porphyromonas gingivalis*. *J Dent Res* 2001;**80**:1425–9.
- Tang-Larsen J, Claesson R, Edlund MB *et al*. Competition for peptides and amino acids among periodontal bacteria. *J Periodontal Res* 1995;**30**:390–5.

Weitz D, Harder D, Casagrande F *et al.* Functional and structural characterization of a prokaryotic peptide transporter with features similar to mammalian PEPT1. *J Biol Chem* 2007;**282**:2832–9.

Table 1. Bacterial strains used in this study.

Bacteria	Strain	Genotype	Source or reference
<i>P. gingivalis</i>	ATCC 33277	–	ATCC
	NDP700	<i>sstT::cepA</i>	This study
	NDP701	<i>sstT::cepA opt::[ermF ermAM]</i>	This study
	NDP702	<i>sstT::cepA pot::[ermF ermAM]</i>	This study
	NDP800	<i>opt::cepA</i>	This study
	NDP801	<i>opt::cepA pot::[ermF ermAM]</i>	This study
	NDP900	<i>pot::cepA</i>	This study
	NDP901	<i>pot::cepA opt::[ermF ermAM]</i>	This study
	<i>E. coli</i>	XL-1 Blue	–
<i>Strep. anginosus</i>	NCTC 10713	–	NCTC

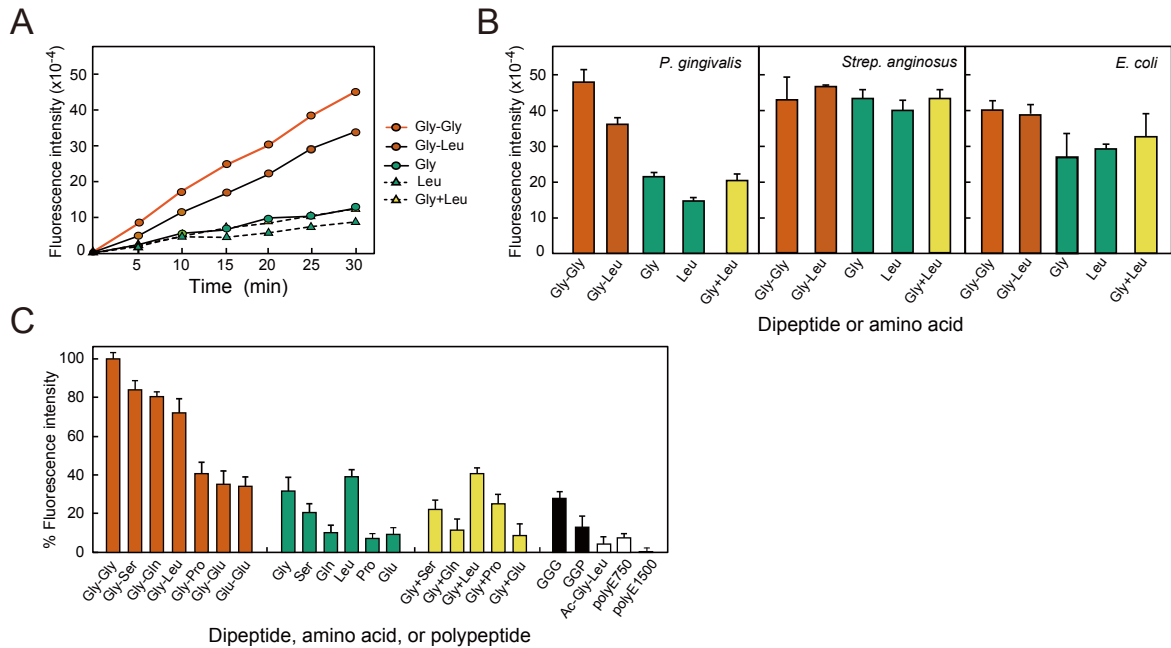


Figure 1. Substrate uptake potential determined by real-time metabolic activity.

(A) Fluorescence intensity was measured with *P. gingivalis* pre-incubated with resazurin reagent with either 5 mM Gly-Gly or Gly-Leu, 10 mM Gly or Leu, or 5 mM each of Gly and Leu. The average was shown. (B) Substrate uptake was measured and fluorescence intensity at 30 min is depicted for *P. gingivalis*, *Strep. anginosus*, and *E. coli*. (C) The analysis with *P. gingivalis* was performed with at identical moles as amino acids (5 mM Gly-Xaa and Glu-Glu, 10 mM single amino acid, 5 mM of each combination of amino acids, 3.3 mM GGG, GGP, 5 mM Ac-Gly-Leu, 1.7 mM poly E750, 0.7 mM polyE1500). Representative results at 30 min are shown as the average \pm S.D. (n = 4), and four independent measurements were performed.

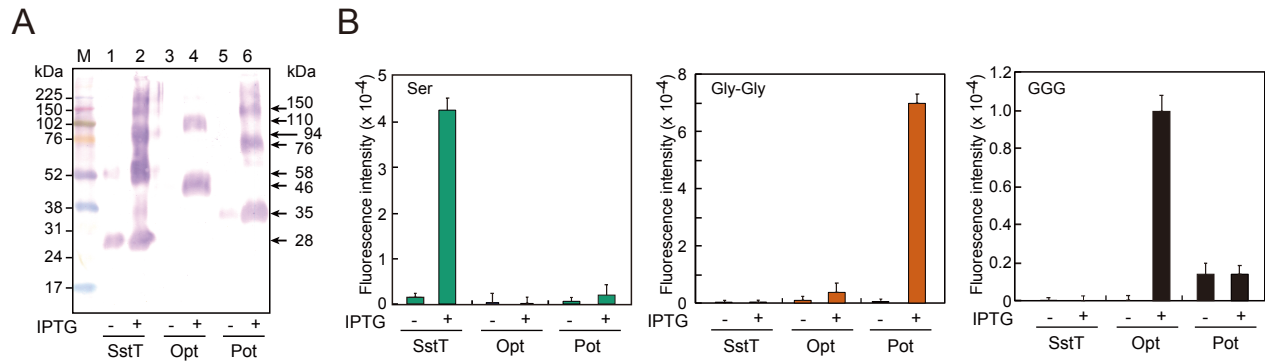


Figure 2. Expression of *P. gingivalis* transporters in *E. coli*.

(A) Western blot analysis of *P. gingivalis* SstT, Opt, and Pot expressed in *E. coli* with pTrcHis2-TOPO-*sstT*-, *opt*, and *pot*, respectively. Whole bacterial cell lysates were subjected to immunoblotting with an anti-hexahistidine Ig. **(B)** *E. coli* cells were cultured with or without IPTG. After washing and preparation of bacterial cell suspensions, substrate uptake was measured with 10 mM Ser, 5 mM Gly-Gly, and 3.3 mM GGG for 30 min. Values were obtained by subtraction of endogenous uptake of *E. coli* without plasmids. Representative results from three independent experiments are shown as the average \pm S.D. (n = 4).

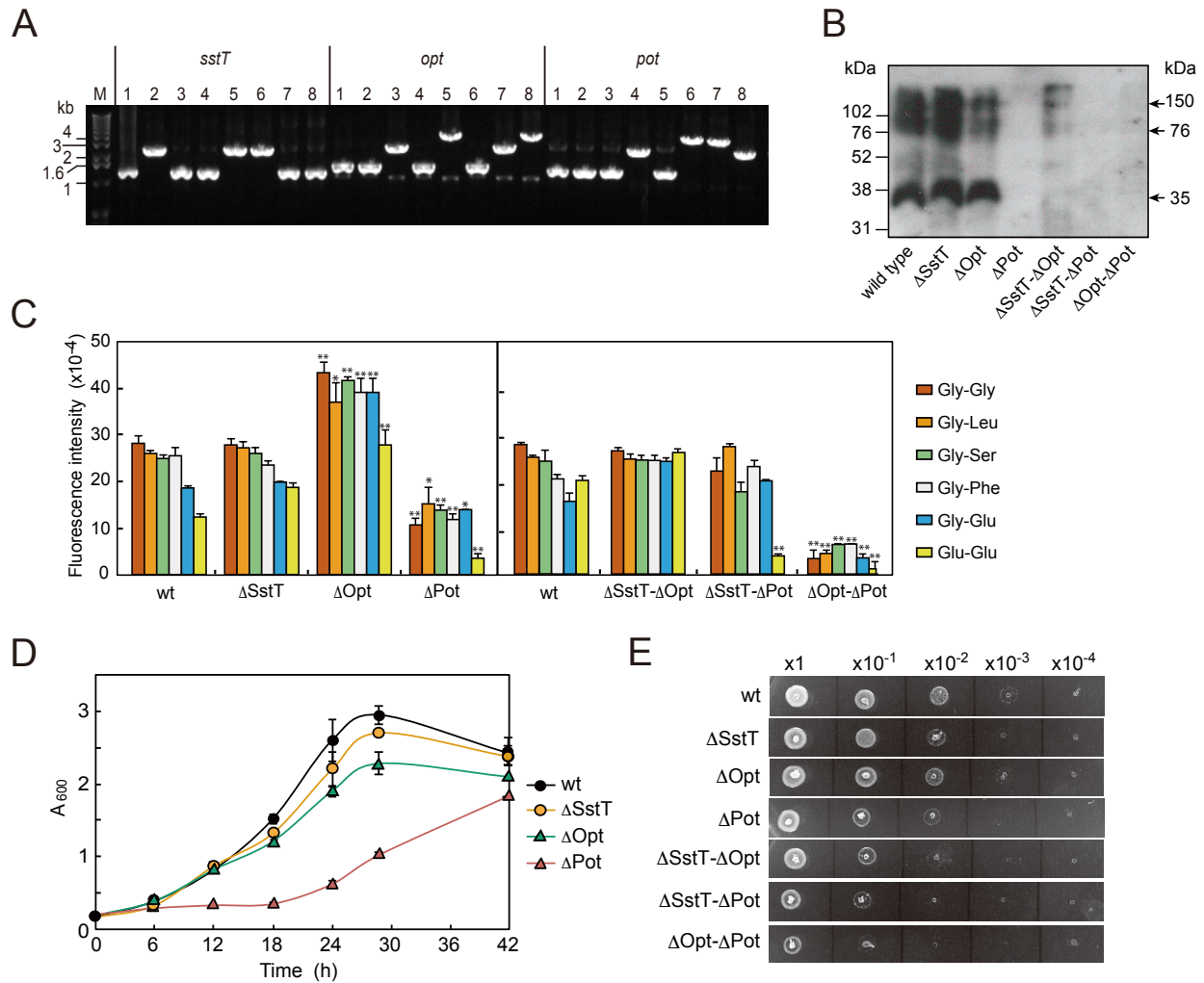


Figure 3. Characteristics of transporter-deficient *P. gingivalis* strains.

(A) Transporter-deficient *P. gingivalis* strains were confirmed by PCR using sets of primers for nested PCR and genomic DNA from wild type (lane 1), Δ *sstT* (lane 2), Δ *opt* (lane 3), Δ *pot* (lane 4), Δ *sstT*- Δ *opt* (lane 5), Δ *sstT*- Δ *pot* (lane 6), Δ *opt*- Δ *pot* (lane 7), and Δ *pot*- Δ *opt* (lane 8). (B) Whole cell lysates (5 μ g of protein) were subjected to SDS-PAGE and *P. gingivalis* Pot was detected with ECL immunoblotting. (C) Dipeptide uptakes were measured by the real-time metabolic assay. Representative results at 30 min are shown as the average \pm S.D. (n = 4), and three independent measurements were performed. * p < 0.05, ** p < 0.01, as compared with wild-type (Student's *t*-test). (D) *P. gingivalis* strains were grown in ABCM broth. The average \pm S.D. was calculated (n = 4). (E) *P. gingivalis* strains at 10^7 cfu 2μ L⁻¹ and 10-fold serially diluted bacterial cell suspensions were inoculated on blood agar plates and cultured for 42 h.

TM helix 1

PgPot	-----MLKNHP-----KGLISASLTMG ERF GFYIMMGILLFLQAKFGLSGKE-----ASVIYS	50
PepTSh	MATNNSHEQTIQSIPOKGFFFGHP-----RGLGVLFV EFWERF SYGMRAMLIFY--MYFAIHQNGLDKTTMSIMS	72
SauPepT	MTQQNSHGNIQDIPQTGFFFGHP-----RGLGVLFV EFWERF SYGMRAILLIFY--MYFAVTNGLDLDKTTMSIMS	72
GkPot	--MASIDKQOIAASVPQRGFFFGHP-----KGLFTLFF TFWERF SYGMRAILVY--MYEVSXKGLGLDEHLALAIMS	71
PepTSt	---MEDKG-----KTFFFGQF-----LGLSTLFMT EWERF SYGMRAILLY--MWFLLISTGDL---HITRATAAS	58
LlDptT	MQNLNKTE-----KTFFFGQF-----RGLLTLF QTEWERF SYGMRAILVYLYALTADNAGLGLPKAQAMAIVS	66
PepTSo	---MSVAKPQ-----GTMLGHP-----KGLFLFF TLWERF SYAMRAILVLYLVQVQKGGGLGWTQADALSLYG	65
EcDtpB	----MNT-----TTPMGM LQ QPRPFMIFV ELWERF GYGVQG-----VLAVFFVKQLGFGSQEQAFVTFG	57

TM helix 2 TM helix 3 TM helix 4

PgPot	IFYASVYVLA LVG ---GIIADSMKNYKGTILVGLIVMAAGYVMLGIPTPTQATGMTPWLIF TC CAALAFIS FNGLFK	124
PepTSh	VYGALIMSSIPG---AWIAD RI TGTRGATLLGAVLII IGHICL ---SLPFALF-----GLFSSMFFIIIG SGLMK	137
SauPepT	VYGLIYMTSIPG---CWIAD RI TGTRGATLLGAVFII IGHICL ---SLPFALI-----GLFSSMFFIIIG SGLMK	137
GkPot	IYGALVMSGI IIG ---GWLAD RV FGTSRAV FV GGLLIMAGHIAL---AIPGVA-----ALFVSMALVIG TGLLK	136
PepTSt	IMAIYASMYVLS GT TIGGFVAD RI IGARPAV FVG GVVIMLGHIVL---ALPFGAS-----ALFGSIIILII IGTGLFK	126
LlDptT	IYGALVYVLS TVG ---CWVAD RL L GA SRTIFL GG ILITLGHIAL---ATPFGLS-----SLFVALFLIIL GTGMLK	131
PepTSo	TFTALVYVLS PLIG ---GWLAD N FLGQRKAIY F GGALMAT GQ FML---AAPHAW FPG IETT VY I GL TLIL GNGLFK	136
EcDtpB	AFAALVYGLIS IG ---GYV GD HLLG TK RTIVL GA LVLAIGY FMTG ---MSLLK PDL IF I AL GT I AV ----- GNGLFK	123

TM helix 5 TM helix 6

PgPot	GNLQALVGRMYDND TY RD KRD SG F SLFYMFIN V GA V FAPLVAVAI---RNWVQ HNG FVYNADL---PER CH QIL-	193
PepTSh	PNISNI VG RLY P END TR IDAG FV IF---YMSVNL GA LIS PI IL QHF ---VDIRNF HGG FL LA IG- MA LGLVWYLL---	206
SauPepT	PNISNI VG RLY P END RR MDAG FV IF---YMSV N MGAL L S PI IL QHF ---VNVKN F HGG F L IA AVG- MA LGLVWYV---	206
GkPot	PNVSS I VG DM Y KP GD DR RDAG F S I F---YMGIN GA F L AP L VV GT A---GMKYN F HL G F LA AVG- M F L GLV V V A ---	205
PepTSt	PNVSTL Y GT LY DE H RR RD AG F S I F---VFGIN GA F I AP L I V GA A ---QEAAG Y H V A F SL AA IG- M F L GL V Y F ---	195
LlDptT	PNISNM VG H L Y S K D S RR DT G FN I F---VVGIN MG S L I A P L I V GT V ---GQGVN Y HL G F S L AA IG- M I F AL F AY W Y---	200
PepTSo	PNISTM VG D L Y E EG D HR RD AG F T I F---YMGIN GA L S GF V V A W A Y T S F G H A E V I NG K EV T N- N W Q AG F F C AG I GM	210
EcDtpB	AN P AS L L S K C Y P PK D PR L D GA F T L F ---YMSIN I GS L I A LS L AP V I A DR F GY S V T YN L CG A GL I I A L V Y I AC R G---	195

HA HB

PgPot	-----NGTLPENAKAQVMEMIQ AA NGT---AVATEGL Q E F AL K YI Q V F S T G F H A F L AA V F M AI	251
PepTSh	-----FNRKNLGSVGMKPT N PL S KE ER K---YGM I IG-----I V AI V IV L LV V Y T HT L	257
SauPepT	-----FNRKNLGSVGMKPT N PL T PA E KK---YGL I IG-----S V LA I VL I IG V AL T NS	256
GkPot	-----TRKKNLGLAG T Y V PN L T PA E KK ---AAA I MA-----V G AV V IA V LL A IL L P NG ---	252
PepTSt	-----GKKTLDPHYLR P TD L AP E V K PL L - V K---V-----SLAVAG F IA I IV M N L V GW	243
LlDptT	-----GRLRH F PE I GR E PS N PM D S K ARR N FL-IT L T V -----V I VA I IG F FL V Y Q AS P AN F	251
PepTSo	LLSL V I Q FL A Q K LL G D I GT V PAAR L ER E R Q AK L GN R KE P L T TK V ER D -----R I K V IM V GL F T I F W AG F	277
EcDtpB	-----MVKD I G S E P DF R PM S F S K L LY V LL G -----S V MI F V C AW L M H N V EV AN	297

TM helix 7

PgPot	SFLI Y I N K H Q Y PAD Q KA-----NA V TE A H K D Q K Q E I K M A D E I R Q R I I A L C A V F G V V I F W M S F H Q NG V S	317
PepTSh	----SFDLIS N TVL V LG V ---AL P II Y FT M L R S K D V T D GE---RS R V K ---AF I PL F IL G M L F W S I Q E Q S N V LN I - Y	320
SauPepT	L---S F NL V S N TVL V LG I ---AL P II Y FT L I R S K D V T D TE---RS R V K ---AF I PL F IL G M V F W A I Q E Q S N V LN I - Y	320
GkPot	----W F T V ET F IS L VG I L G II I PI I Y F V V MY R SP K T A E B ---RS R V I ---AY I PL F V A S A M F W A I Q E Q S T IL A N - Y	319
PepTSt	----NSL P AY I N L L T I V A---IA P V F Y F AW M IS S V K T S T E -HL R V V ---SY I PL F IA V L F W A IE Q S V LV L AT F A	310
LlDptT	I---NN F IN V LS I IG I V V ---P I I---Y F VM M F T SK V ES D E---RR K L T ---AY I PL F LS A IV F W A IE Q S S T I AV - W	315
PepTSo	E Q A---G L M N L F T N E F T D R-----Y I G T W E V P T T Y F Q---SL N AI---F I V L F A P V V A S I W I R---L G K N E P NS P V	337
EcDtpB	L-----V L IV L S I V V T-----I I FF R Q A FK L D K T G R N K---M F V A F---V L M L E A V V F Y I L Y A Q M P T SL N F F AI---	297

TM helix 8 TM helix 9

PgPot	LT Q FA K D Y IDL S S V K L DL G -F T S I V G A E M F Q S IN P FF V VT L PL L LL F IF G FL K ---RN M E P ST P K I VI G M F IA L	390
PepTSh	GL E R S DM Q LN L F G W T TR F GE A L F Q S IN L FL L F A P V IS M I W ---L K ---M G K Q P S L A IK F S I GT L LAG L	385
SauPepT	GI E H S DM K LN L F G W K T N F G E A IF Q S I N L FL I LL A PI S LL W -----Q K ---L G T K Q P SL P V K F A IG T FL A G A	385
GkPot	A---DK R I Q LD---V A GI H LS P AW F Q S L N PL F II L AP V FA W W---V K ---L G K R Q P T I PO K F A L G LL F AG L	380
PepTSt	A E R V D S W F FP V -----S W F Q S L N L PL F IM L Y T PF A W L W-----T A ---W K KN Q PS S PT K F A V G L M F A GL	366
LlDptT	GE S R S N L D P T W F G IT F H I D S W Y Q L L N PL F I V LL S PI F VR L W-----N K ---L G ER Q P S T I V K F L GL M L T GI	380
PepTSo	K F -AL G LV L LA I GL F LM I GA V VE-----M G D-----A S ---A K S S -----M W W L V G A Y F F H T M	382
EcDtpB	---NN V H H E I L---G F S I N P V S F Q AL N PF V V L AS P IL A GI Y -----T H L G N K G K D L S M PM K F T L G M F M C S L	358

TM helix 10

PgPot	AF V VM A IG S M GL PT F E R N A GV E ----F T K V SP W ML V TY M IL T IA L EL F IS PM G I S F V S K V AP H L Q IG M Q L W L C	462
PepTSh	SY I L I GL V GL-----G Y G H T-----Q F S V N---W V IL S Y V IC V IG L CL S PT G NS A AV K L A P K AF N A Q M M S V W L L	447
SauPepT	SY I L I GL V GY-----A S G S S-----N F S V N---W V IL S Y I IC V IG L CL S PT G NS A AV K L A P K AF N A Q M M S I W L	447
GkPot	S F I---V I LP-----G H LS G -----G L W H PI W L V SY F IV V L G EL CL SP V GL S AT T K L AP A F S A Q T M SL W FL	442
PepTSt	S F LL M A I PG A -----L Y GT S -----G - K V SP L W L V G S W AL V IL G ML I SP V GL S VT T K L AP K AF N S Q M S M W FL	429
LlDptT	SY L IM L TP L GL-----L N GT S -----G - R A S A L W L V LM F AV Q MA L LL V SP V GL S V S T K L A P V A F Q S M A M W FL	450
PepTSo	G E L C LS P IG L -----S M V T K L AP L R I AS L MM G AW L FL V AA N K I GG V VG S F I GH G GE K E Q L A N A M I F S GI A IT	452
EcDtpB	G F L T AA A AG M -----W F AD A -----Q G L T SP W F I V L V L F Q SL G EL F I S AL G L A M I A A L V P Q H L M G F I L G M W FL	422

TM helix 11 TM helix 12

PgPot	ATA-----V G NS L LF V GM I LY S L-----S I S A T W I V F T CA C ALS M L V ML S M V K W L E R V - A K-----	513
PepTSh	T-----N A S A Q A IN G TL V K L IK P L-----G Q T N Y F IF L GT V AI V I T LI L IV S F S PT K A-M K GI H -	501
SauPepT	T-----N A S A Q A IN G TL V K L IE P L-----G Q T N Y F IF L GT V AI V I T IV L AI S PL I IK A -M K GI R -	501
GkPot	S-----N A AA Q A I NA Q L V RF Y TP E -----N E T A Y F GT I GG A L V L G IL L AI A P R I G RL-M K GI R -	496
PepTSt	S-----S S VG S AL N A Q L V T L Y N A K -----S E V A Y F S Y FG L S V VL G IV L V F LS K R I Q L -M Q GV E -	483
LlDptT	A-----D S T S Q A INA Q IT PL FK A A-----T E V H FF A IT G I I GI V GI L L V KK P IL L K - MG D V R -	497
PepTSo	A-----A L S G V I Y F M A D K L V D-----W M H G A E S K H H NE A E A L E A E I A V T A E H E A - IK R ---	500
EcDtpB	T Q AA F LL G GY V AT F T A VP D NI D PLE T LP V Y T N V FG K I G L V TL G V A V M LL M V P L K R M IA T P E S H	489

Figure 4. Sequence alignment of the POT family members and secondary structure of *P. gingivalis* Pot. Amino acid sequences of *P. gingivalis* Pot (PgPot, UniProt: B2RH09), *Staphylococcus hominis* PepT_{Sh} (A0A533J3Z5), *Staphylococcus aureus* SauPepT (A0A0H2XIN4), *Geobacillus kaustophilus* GkPot (Q5KYD1), *Streptococcus thermophilus* PepT_{St} (Q5M4H8), *Lactococcus lactis* LiDptT (P0C2U2), *Shewanella oneidensis* PepT_{So} (K4PU14), and *E. coli* DtpB (P36837) were aligned. Identical residues in 8 and 7 molecules are highlighted in yellow and green, respectively, and essential amino acid residues in the conserved ExxER/K motif and 5 residues involved in H⁺-driven substrate uptake proposed for GkPot are presented in bold red. Transmembrane (TM) helices, additional intermediate helix A (HA) and HB, and α -helices in black are indicated within the sequences predicted by Phyre2 modeling.

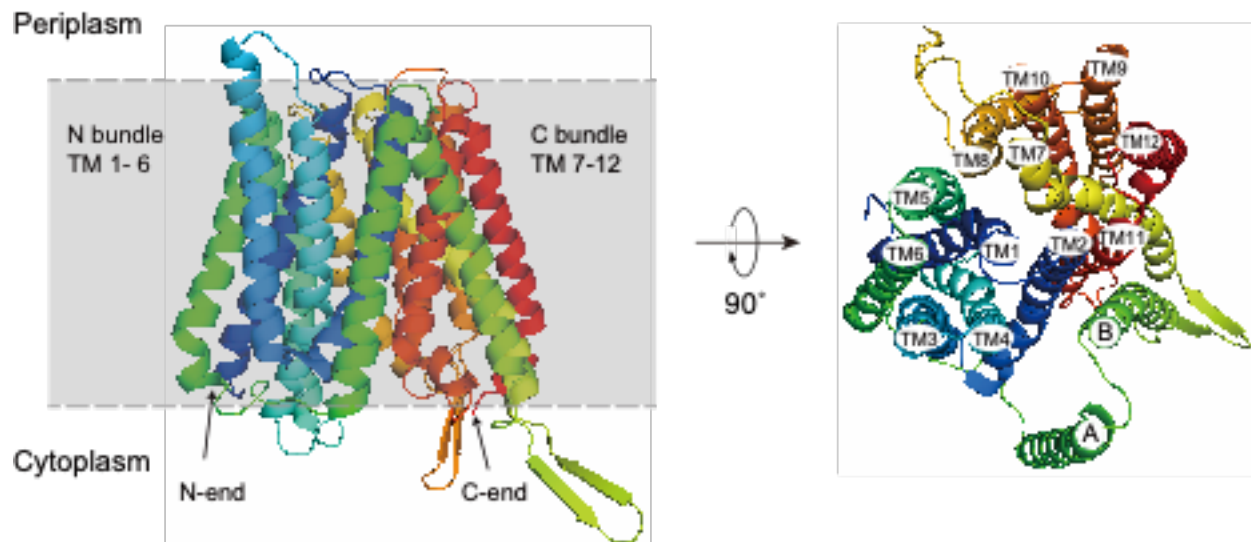


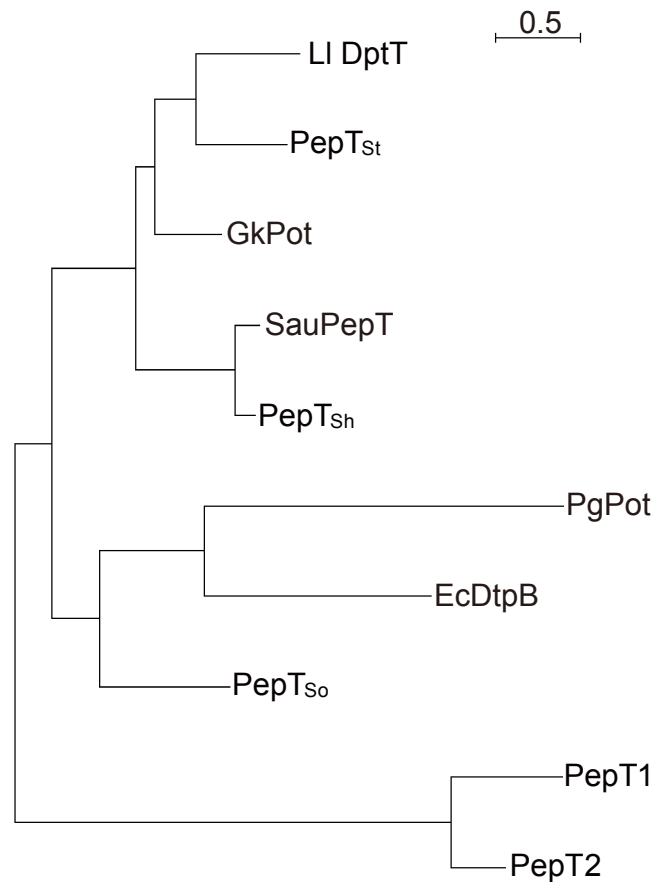
Figure 5. 3D homology modeling of *P. gingivalis* Pot.

A 3D homology model was generated by Phyre2 in the plane of the inner membrane. The canonical N bundle of TM 1 – 6 and C bundle of TM 7 – 12, with additional intermediate helix A (A) and helix B (B), are indicated.

Supplemental Table S1. Primers used in this study.

Usage	Name	Sequence (5'-3')
<i>sstT</i> 5' fragment- <i>cepA</i>	PGN1640-5F1* ¹	atgcgtaaactacggatcggcctct
	PGN1640-5R- <i>cep</i> -comp	TGCTTCACACtggcaatgaatcctgccaccg
<i>sstT</i> - <i>cepA</i>	PGN1640-5F- <i>cepF</i>	gattcattgccaGTGAAGCATCTTCGATGCTG
	PGN1640-3R-comp	aaggattcttctCCGATAGTGATAGTGAACGG
<i>sstT</i> 3' fragment- <i>cepA</i>	<i>cep</i> -3F-PGN1640-3F	TCACTATCGGagaagaatccttcaggatgc
	3R-comp-PGN1640	cgggcagacataactcgcgcatcc
<i>sstT</i> nested PCR	PGN1640-5F2	ttgcccaagatcatattgg
	3R-comp-2-PGN1640	agagagggatcgtaaagcc
<i>opt</i> 5' fragment- <i>cepA</i>	PGN1518-5F1* ²	tcatcggcggttctcctcggtatatt
	PGN1518-5R- <i>cep</i> -comp	TGCTTCACACaaaagcatcgttaccaccaaa
<i>opt</i> - <i>cepA</i>	PGN1518-5F- <i>cepF</i>	aacgatgcttttGTGAAGCATCTTCGATGCTG
	PGN1518-3R-comp	ttgaattggaagCCGATAGTGATAGTGAACGG
<i>opt</i> 3' fragment- <i>cepA</i>	<i>cep</i> -3F-PGN1518-3F	TCACTATCGGcttccaattcaactgctgtt
	3R-comp-PGN1518* ³	ttatgcttcatgtttcttgcctctg
<i>opt</i> nested PCR	PGN1518-5F2	tgctattgattccttccg
	3R-comp-2-PGN1518	gtcgacgatgaagtagagaat
<i>opt</i> 5' fragment- <i>erm</i>	PGN1518-5F1* ²	tcatcggcggttctcctcggtatatt
	PGN1518-5R- <i>erm</i> -comp	CAATAGCGGAAGCTaaaagcatcgttaccaccaaa
<i>opt</i> - <i>erm</i>	PGN1518-5F- <i>ermF</i>	aacgatgcttttAGCTTCCGCTATTGCTTTTTTTC
	PGN1518-3R-comp- <i>erm</i>	ttgaattggaagCTCTAGAGGATCCCCGAAGCTG
<i>opt</i> 3' fragment- <i>erm</i>	<i>erm</i> -3F-PGN1518-3F	GATCCTCTAGAGcttccaattcaactgctgtt
	3R-comp-PGN1518* ³	ttatgcttcatgtttcttgcctctg
<i>pot</i> 5' fragment- <i>cepA</i>	PGN0135-5F1* ⁴	atcttctatgcttcggtatattgtattg
	PGN0135-5R- <i>cep</i> -comp	TGCTTCACACaactcgcgcaaagagcaataat
<i>pot</i> - <i>cepA</i>	PGN0135-5F- <i>cepF</i>	ctttgcgagttGTGAAGCATCTTCGATGCTG
	PGN0135-3R-comp	aacgacaccgaaCCGATAGTGATAGTGAACGG
<i>pot</i> 3' fragment- <i>cepA</i>	<i>cep</i> -3F-PGN0135-3F	TCACTATCGGttcgggtcgttattttctc
	3R-comp-PGN0135* ⁵	ttacttcgctaccgctccagccac
<i>pot</i> nested PCR	PGN0135-5F2	tgggctctcgtggaggta
	3R-2-PGN0315	aacctggagagcataacgag
<i>pot</i> 5' fragment- <i>erm</i>	PGN0135-5F1* ⁴	atcttctatgcttcggtatattgtattg
	PGN0135-5R- <i>erm</i> -comp	CAATAGCGGAAGCTaactcgcgcaaagagcaataat
<i>pot</i> - <i>erm</i>	PGN0135-5F- <i>ermF</i>	ctttgcgagttAGCTTCCGCTATTGCTTTTTTTC
	PGN0135-3R-comp- <i>erm</i>	aacgacaccgaaCTCTAGAGGATCCCCGAAGCTG
<i>pot</i> 3' fragment- <i>erm</i>	<i>erm</i> -3F-PGN0135-3F	GATCCTCTAGAGttcgggtcgttattttctc
	3R-comp-PGN0135* ⁵	ttacttcgctaccgctccagccac

<i>sstT</i> expression	PGN1640-5F1* ¹	atgcgtaaactacggatcggcctct
	3R-PGN1640-comp	ccttgcgactgcttgcctcttgegc
<i>opt</i> expression	5F-PGN1518	atggaaaacaacagacaacgagcat
	3R-PGN1518-comp	tgctcatgtttcttgcctctgatgctgtc
<i>pot</i> expression	5F-PGN0135	atgctaaagaatcacccctaaagggttaatctc
	3R-PGN0135-comp	cttcgctaccgctccagccactta



Supplemental Figure S1. Phylogenetic tree of the POT family members.

A phylogenetic tree of *P. gingivalis* POT and bacterial homologues shown in Fig. 4 and human homologues was created using the PhyML package with default settings following sequence alignment with Clustal W. *P. gingivalis* PgPot (UniProt: B2RH09), *Staphylococcus hominis* PepT_{Sh} (A0A533J3Z5), *Staphylococcus aureus* SauPepT (A0A0H2XIN4), *Geobacillus kaustophilus* GkPot (Q5KYD1), *Streptococcus thermophilus* PepT_{St} (Q5M4H8), *Lactococcus lactis* LiDptT (P0C2U2), *Shewanella oneidensis* PepT_{so} (K4PU14), *E. coli* DtpB (P36837), *Homo sapiens* PepT1 (O43641) and PepT2 (S15A2).